AFGL-TR-88-0105
ENVIRONMENTAL RESEARCH PAPERS, NO. 1001

Possible Measurement Errors in Calibrated AVHRR Data

ROBERT PAUL d'ENTREMONT
THOMAS J. KLEESPIES

1 April 1988

ATMOSPHERIC SCIENCES DIVISION PROJECT 6670
AIR FORCE GEOPHYSICS LABORATORY
HANSCOM AFB, MA 01731

"This technical report has been reviewed and is approved for publication."

FOR THE COMMANDER,

Kenneth R. Hardy

KENNETH R. HARDY, Chief
Satellite Meteorology Branch

Donald A. Chisholm

DONALD A. CHISHOLM, Acting Director
Atmospheric Sciences Division

This document has been reviewed by the ESD Public Affairs Office (ESD/PA) and is releasable to the National Technical Information Service (NTIS).

Qualified requestors may obtain additional copies from the Defense Technical Information Center. All others should apply to the National Technical Information Service.

If your address has changed, or if you wish to be removed from the mailing list, or if the addressee is no longer employed by your organization, please notify AFGL/DAA, Hanscom AFB, MA 01731-5000. This will assist us in maintaining a current mailing list.

Do not return copies of this report unless contractual obligations or notices on a specific document require that it be returned.

Unclassified

SECURITY CLASSIFICATION OF THIS PAGE

REPORT DOCUMENTATION PAGE

1a. REPORT SECURITY CLASSIFICATION	1b. RESTRICTIVE MARKINGS
2a. SECURITY CLASSIFICATION AUTHORITY	3 DISTRIBUTION / AVAILABILITY OF REPORT Approved for Public Release; Distribution Unlimited
2b. DECLASSIFICATION / DOWNGRADING SCHEDULE	
4. PERFORMING ORGANIZATION REPORT NUMBER(S) AFGL-TR-88-0105 ERP, No. 1001	5. MONITORING ORGANIZATION REPORT NUMBER(S)
6a. NAME OF PERFORMING ORGANIZATION: Air Force Geophysics Laboratory 6b. OFFICE SYMBOL (If applicable): LYS	7a. NAME OF MONITORING ORGANIZATION
6c. ADDRESS (City, State, and ZIP Code) Hanscom AFB Massachusetts 01731-5000	7b. ADDRESS (City, State, and ZIP Code)
8a. NAME OF FUNDING / SPONSORING ORGANIZATION: Air Force Geophysics Laboratory 8b. OFFICE SYMBOL (If applicable): LYS	9 PROCUREMENT INSTRUMENT IDENTIFICATION NUMBER
8c. ADDRESS (City, State, and ZIP Code) Hanscom AFB Massachusetts 01731-5000	10. SOURCE OF FUNDING NUMBERS PROGRAM ELEMENT NO: 62101F; PROJECT NO: 6670; TASK NO: 17; WORK UNIT ACCESSION NO: 07

11. TITLE (Include Security Classification)
Possible Measurement Errors in Calibrated AVHRR Data

12. PERSONAL AUTHOR(S)
d'Entremont, Robert Paul, Kleespies, Thomas J.

13a. TYPE OF REPORT	13b. TIME COVERED	14. DATE OF REPORT (Year, Month, Day)	15. PAGE COUNT
Scientific, Interim	FROM 1987 TO 1988	1988 April 1	26

16. SUPPLEMENTARY NOTATION

17. COSATI CODES			18. SUBJECT TERMS (Continue on reverse if necessary and identify by block number)
FIELD	GROUP	SUB-GROUP	Remote Sensing; Weather Satellites; Satellite Data Calibration; Cloud Analysis; NOAA AVHRR

19. ABSTRACT (Continue on reverse if necessary and identify by block number)

Visible and infrared meteorological satellite data are a primary source of global cloud observations. Such data are calibrated in order to provide its users with a method for converting from "raw" measurements, called counts, to physically sensible measurements such as albedo or brightness temperature. This report describes the procedure for converting National Oceanic and Atmospheric Administration Advanced Very High Resolution Radiometer (NOAA AVHRR) raw counts to albedos and brightness temperatures. This procedure involves the use of "calibration coefficients", that help define the relationship between the raw counts and the physical measurements they represent. Such relationships are referred to as "look-up-tables".

In theory, calibration coefficients (and therefore look-up tables) do not change noticeably from one scanline of satellite data to the next. This makes feasible the generation of a constant look-up table that can be used over long periods of time for all data. In practice, calibration coefficients can and often do change from one scan to the next. These changes imply accuracy

(Continued)

20. DISTRIBUTION / AVAILABILITY OF ABSTRACT	21. ABSTRACT SECURITY CLASSIFICATION	
☐ UNCLASSIFIED/UNLIMITED ☒ SAME AS RPT ☐ DTIC USERS	Unclassified	
22a. NAME OF RESPONSIBLE INDIVIDUAL: Robert P. d'Entremont	22b TELEPHONE (Include Area Code): (617) 377-3498	22c. OFFICE SYMBOL: LYS

DD FORM 1473, 84 MAR — 83 APR edition may be used until exhausted. All other editions are obsolete.

SECURITY CLASSIFICATION OF THIS PAGE
Unclassified

Block 19. (Continued)

errors in measured brightness temperatures that are significant for some satellite data analysis algorithms; others are less severely affected.

This report addresses the potential errors that can be expected when using constant look-up tables, i.e., by assuming that sensor calibration does not change from one scanline to the next.

Contents

Illustrations

Tables

Possible Measurement Errors In Calibrated AVHRR Data

1. INTRODUCTION

The NOAA Advanced Very High Resolution Radiometer (AVHRR) is a scanning radiometer that simultaneously senses reflected sunlight and and emitted thermal infrared energy in the five "channels," or window regions, listed in Table 1 (some AVHRR instruments do not contain Channel 5; NOAA-10 is the last AVHRR instrument to be flown without Channel 5). Channels 1 and 2 sense reflected solar energy and are used to detect cloud cover, snow cover, and sea ice, along with cyclones and volcanic dust plumes. Clouds reflect sunlight equally well in both the visible Channel 1 and the near-infrared Channel 2. However, land backgrounds reflect visible light poorly when compared with the near-infrared. Land backgrounds that appear dark in the visible imagery appear bright in the near-infrared imagery. This is helpful for clear/cloud distinctions and to automated cloud analyses such as the Air Force Global Weather Central's Real-time Nephanalysis (AFGWC RTNEPH) because most backgrounds will have a different spectral signature than clouds. Thus the use of Channel 1 and Channel 2 data can alleviate the dependency of the RTNEPH on background brightness fields.

At night, the infrared Channel 3 sensor of the AVHRR measures thermal energy in the 3.7μm wavelength region. Channel 3 was chosen to complement Channel 4 in the remote sensing of sea surface temperatures by providing corrections to Channel 4 temperature measurements contaminated by partial cloud cover and atmospheric water vapor. Atmospheric water vapor is a weak absorber at 3.7μm. Consequently, thermal energy emitted at Channel 3 wavelengths by surfaces such as land, the ocean,

Table 1. Spectral Intervals for the Five NOAA-7 AVHRR Window Channels

Five-Channel NOAA-7 AVHRR				
Channel 1	Channel 2	Channel 3	Channel 4	Channel 5
0.58-0.68μm	0.725-1.1μm	3.55-3.93μm	10.3-11.3μm	11.5-12.5μm

and clouds can penetrate larger amounts of water vapor without being attenuated. Thermal energy emitted at the longer Channel 4 wavelengths can not penetrate water vapor as effectively. On the other hand, incident solar radiance at Channel 3 wavelengths is not negligible, as it is at Channel 4 wavelengths. Reflected sunlight is often a significant part of daytime Channel 3 radiance measurements, and can be as large as emitted terrestrial radiances. Channel 3 nighttime imagery has characteristics similar to imagery from the longer-wavelength infrared Channels 4 and 5. Channel 3 imagery can help the RTNEPH to discriminate low clouds and fog from clear land/ocean, and to detect thin cirrus.

Channel 4 senses emitted thermal energy, and is therefore used for the mapping of thermal radiation emitted by clouds, the earth's surface, and oceans during both day and night. Even though Channel 4 is an atmospheric window region, radiation emitted at Channel 4 wavelengths is noticeably affected by water vapor. Water vapor is the main tropospheric absorber of radiation at these wavelengths, and significantly attenuates emitted thermal radiation. Channel 5 also senses emitted thermal energy and has the same characteristics as Channel 4, except that Channel 5 radiation is even more sensitive to water vapor. Corresponding measured brightness temperatures from both channels are similar for clear, cold atmospheres since usually such atmospheres are quite dry. But due to attenuation by atmospheric water vapor, Channel 5 brightness temperatures are as much as 3 percent lower than their corresponding Channel 4 temperatures when measured in moist atmospheres. Channels 4 and 5 data used together can provide cloud analysis models such as the RTNEPH with atmospheric water vapor attenuation corrections to satellite-measured brightness temperatures.

It is the intent of this report to provide AFGWC with information on how AVHRR data are measured and calibrated, how this data can be most effectively and precisely used, and to help develop an improved understanding of the accuracy and precision that can be expected of the calibrated data. The AVHRR sends down 10-bit "raw count" values for each of the five channels. The raw visible counts (Channels 1 and 2) may be converted to normalized albedoes, and the raw infrared counts (Channels 3 and 4, and 5 when present) may be converted to brightness temperatures using "calibration coefficients." Calibration coefficients are provided for each channel individually as a regular part of the data stream, and can change every Global Area Coverage scan (GAC scans contain 4 km data) or every five Local Area

Coverage/High Resolution Picture Transmission scans (LAC/HRPT scans contain 1 km data). Scan-to-scan changes are most noticeable for Channels 3, 4, and 5. A brief description of the procedure for converting the raw counts to albedoes/temperatures is given in Section 1. The variability is discussed of the calibration coefficients on a line-by-line and orbit-by-orbit basis, along with the associated effects on the "look-up tables" used to convert from counts to albedoes/temperatures. In Section 2 the consequences of truncating 10-bit raw counts to 8-bit, 7-bit, or 6-bit counts is discussed. Section 3 summarizes the conclusions of Sections 1 and 2 and discusses the consequences of using "constant" look-up tables and of truncating the original 10-bit raw data stream.

2. AVHRR CALIBRATION PROCEDURES

2.1 Visible Data Calibration

Calibration coefficients are provided for Channels 1 and 2 in the form of "slope" and "intercept" values. Normalized albedoes are a linear function of the measured 10-bit count value and of these slope and intercept values. However, the slope and intercept values provided must first be scaled by 2^{30} and 2^{22}, respectively, before they can be properly used to convert from count to albedo.

Having scaled the slope and intercept values, they may now be used to convert the AVHRR visible count data values to normalized albedo. The percent albedo A is computed as a linear function of the count value, given by

$$A_j = m_j C + b_j, \quad (j = 1,2), \qquad (1)$$

where A_j is the percent albedo measured by Channel j; m_j is the scaled slope value for Channel j in units of percent albedo/count; C is the measured visible 10-bit count value for Channel j; and b_j is the intercept value for Channel j in units of percent albedo.

Figure 1 contains sample plots of look-up tables for converting counts to normalized albedoes for Channels 1 and 2. Note that as the count C increases, the albedo increases as well.

For the NOAA-K, -L, and -M spacecraft (scheduled for the early 1990's) the normalized albedo look-up table will be piecewise linear, consisting of two functions similar to Eq. (1) for each visible channel. One linear relationship will be for the lower albedoes, and the second relationship for the higher albedoes; they will be chosen so as to provide the finest albedo resolution for the darkest scenes.

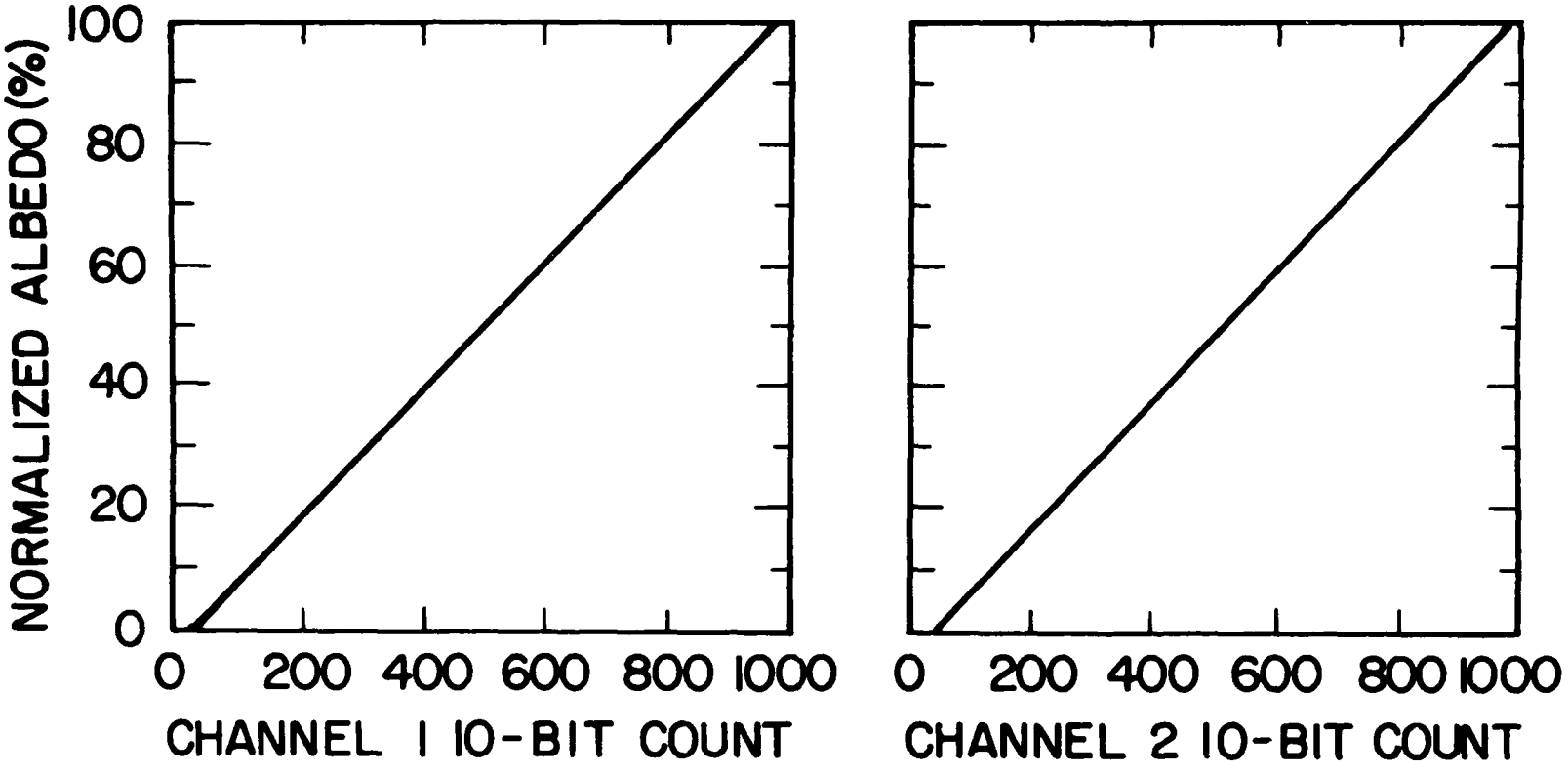

Figure 1. Plots of Look-up Tables for Converting Counts to Normalized Albedoes for Channels 1 and 2

2.2 Infrared Data Calibration

Calibration coefficients are provided for Channels 3 and 4 (and 5 when present) in the form of "slope" and "intercept" values. Emitted thermal energy (in radiance units of $mW/(m^2\ ster\ cm^{-1})$) is a linear function of the measured 10-bit count value and of these slope and intercept values. However, the slope and intercept values provided with each scan line must first be scaled by 2^{30} and 2^{22}, respectively, before they can be properly used to convert from count to radiance and finally to brightness temperature.

Having scaled the slope and intercept values, they may now be used to convert the AVHRR thermal count data values to radiance. The radiance is computed as a linear function of the count value, given by

$$I_j = m_j C + b_j, \quad (j = 3,4,5), \qquad (2)$$

where I_j is the emitted upwelling thermal radiance measured by Channel j; m_j is the scaled slope value for Channel j in units of $mW/(m^2\ ster\ cm^{-1})$ per count; C is the measured thermal 10-bit count value for Channel j; and b_j is the intercept value for Channel j in units of $mW/(m^2\ ster\ cm^{-1})$.

Once the radiance is computed for thermal Channel j, it may then be converted to brightness temperature by inverting Planck's function. The Planck function relates monochromatic radiance with wavenumber (wavelength) and the temperature of the emitting surface. It can be written as

$$B(\nu,T) = \frac{c_1 \nu^3}{e^{\frac{c_2 \nu}{T}} - 1}, \qquad (3)$$

where B is the blackbody Planck radiance; ν is the wavenumber in cm^{-1}; T is the temperature of the emitting surface in °K; and c_1 and c_2 are constants: $c_1 = 1.1910659 \times 10^{-5}\ mW/(m^{-2}\ ster\ cm^{-4})$ and $c_2 = 1.438833$ cm °K. Blackbody radiance increases with temperature, and the wavenumber of maximum radiance increases with increasing temperature.

Inverting Planck's function for temperature yields

$$T[B(\nu,T)] = \frac{c_2 \nu}{\ln\left[1 + \frac{c_1 \nu^3}{B(\nu,T)}\right]}. \qquad (4a)$$

Note that Eq. (4a) gives a form for temperature as a function of radiance B and wavenumber ν. Thus, given a radiance measurement $I_j(C)$ (Eq. (2)) for thermal

Channel j, the equivalent blackbody brightness temperature can be computed using I_j in place of B in (4a):

$$T[I_j(C)] = \frac{c_2 \nu_j}{\ln\left[1+\frac{c_1 \nu_j^3}{I_j(C)}\right]}. \qquad (4b)$$

The "central wavenumber" ν_j is a function of the AVHRR thermal Channel number j, and varies from satellite to satellite. There is some error incurred when using a constant ν_j, due to details of the sensitivity of the sensor itself to upwelling thermal energy. The use of a constant, single ν_j to represent the complete channel j bandwidth is not exact; Eq. (4b) is exact only when ν_j is allowed to vary with radiance. This variation is not large, however, being is greatest for Channel 3.

Nominally, for the NOAA-7 AVHRR, $\nu_3 \simeq 2671$ cm^{-1} for Channel 3, $\nu_4 \simeq 927$ cm^{-1} for Channel 4, and $\nu_5 \simeq 841$ cm^{-1} for Channel 5; these are the values used for this study. More detailed information on each Channel's central wavenumber is always available from (the most recent version of) the NOAA Polar Orbiter User's Guide (Kidwell, 1985). It is important to remember that the temperatures obtained using (4b) are not corrected for atmospheric attenuation.

Equation (4b) can be rewritten in the following form which shows brightness temperature T as a function of the 10-bit count C explicitly. Replacing I_j with (2) in Eq. (4b) yields

$$T_j(C) = \frac{c_2 \nu_j}{\ln\left[1+\frac{c_1 \nu_j^3}{m_j C+b_j}\right]}, \qquad (4c)$$

where m_j and b_j are as for Eq. (2).

Figure 2 contains sample plots of look-up tables for converting counts to brightness temperatures for Channels 3, 4, and 5. Note that as the count C increases, the brightness temperature decreases.

2.3 Variability of Calibration Coefficients

The calibration coefficients can change every GAC scan line, as mentioned in the introductory section; this implies the look-up tables can change from scan to scan as well. A simple statistical analysis was performed to obtain an estimate of the variability of these look-up tables on a scan-by-scan basis. Calibration coefficients for 53497 GAC scan lines were sampled from the NOAA-7 AVHRR, representing ~8 half-orbits in the northern hemisphere for 11 June 1982. These coefficients were then

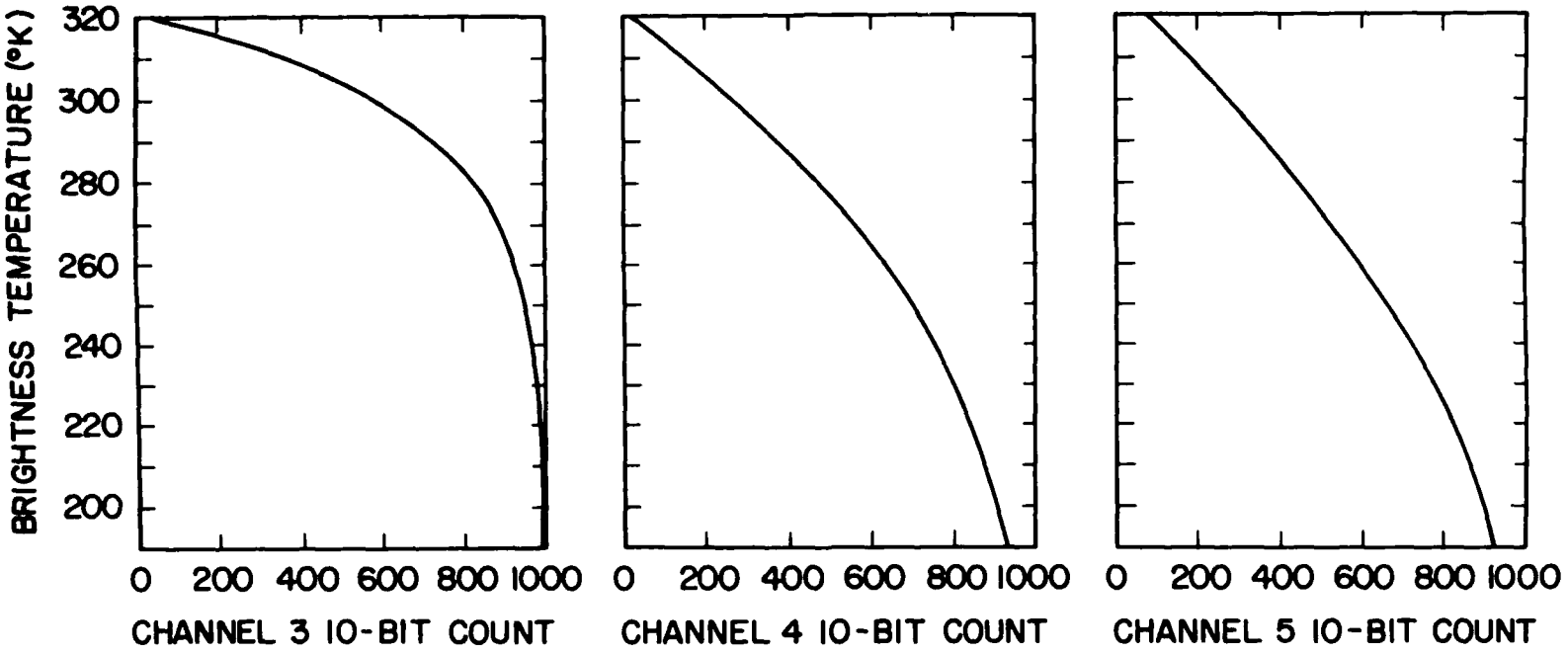

Figure 2. Plots of Look-up Tables for Converting Counts to Brightness Temperatures for Channels 3, 4, and 5

used to generate look-up tables for each channel on a scan-by-scan basis.

For the visible channels, the mean and standard deviation was computed for the 53497 albedo-vs-count look-up tables (one look-up table for each scan line). For the thermal channels, the mean and standard deviation was computed for the 53497 brightness-temperature—vs—count look-up tables (one look-up table for each scan line). The average curves were then tabulated along with their "standard-deviation—envelopes." This analysis was done in order to obtain an estimate of the magnitude of error incurred by using a constant look-up table to convert raw counts to normalized albedoes or brightness temperatures. Results are discussed in the following sections.

2.3.1 VISIBLE CALIBRATION COEFFICIENTS

For each of the 53497 GAC scan lines, a look-up table as given by Eq. (1) was calculated. Then the mean and standard deviation of the albedoes as a function of 10-bit count C were computed. The mean is defined as

$$<A_j(C)> = \frac{1}{N} \sum_{n=1}^{N} A_{j,n}(C), \qquad (5a)$$

and the standard deviation as

$$\sigma_{A_j}(C) = \left\{ \frac{1}{N} \sum_{n=1}^{N} [A_{j,n}(C) - <A_j(C)>]^2 \right\}^{1/2}, \qquad (5b)$$

where N = 53497 GAC scan lines; n is the GAC scan line number (n = 1,2,3,...,53497); $A_{j,n}(C)$ is the albedo look-up value for 10-bit count C, GAC scan line n; and j is the Channel number 1 or 2.

Figure 1 contains plots of the normalized-albedo—vs—counts average look-up tables $<A_j(C)>$ for Channels 1 and 2. Table 2 contains the means (from (5a)) as a function of count for Channels 1 and 2; the standard deviations σ_{A_j} (as defined by (5b)) for all counts are equal to zero out to three places to the right of the decimal, indicating that no appreciable error is to be expected in using constant look-up tables for the "visible" Channels 1 and 2.

2.3.2 INFRARED CALIBRATION COEFFICIENTS

For each of the 53497 GAC scan lines, a look-up table as given by Eq. (4c) was calculated. Then the mean and standard deviation of the brightness temperatures as a function of 10-bit count C were computed. The mean is defined as

$$<T_j(C)> = \frac{1}{N} \sum_{n=1}^{N} T_{j,n}(C), \qquad (6a)$$

Table 2. Average Look-up Table for NOAA-7 AVHRR Channel 1. The mean albedo $<A(C)>$ is given by Eq. (5a) for j = 1,2

NOAA-7 AVHRR Channels 1 and 2 Normalized Albedo Look-up Table		
Mean Albedo (%) $<A(C)>$	Channel 1 10-bit Count C	Channel 2 10-bit Count C
0	33	33
5	79	79
10	126	126
15	173	173
20	219	220
25	266	267
30	313	313
35	360	360
40	407	407
45	454	454
50	500	500
55	547	547
60	594	594
65	641	641
70	688	687
75	734	734
80	781	781
85	828	828
90	875	875
95	921	921
100	968	968

and the standard deviation as

$$\sigma_{T_j}(C) = \left\{ \frac{1}{N} \sum_{n=1}^{N} [T_{j,n}(C) - <T_j(C)>]^2 \right\}^{1/2}, \qquad (6b)$$

where N = 53497 GAC scan lines; n is the GAC scan line number (n = 1,2,3,...,53497); $T_{j,n}(C)$ is the temperature look-up value for 10-bit count C, GAC scan line n; and j is the Channel number 3, 4, or 5.

Figure 2 contains plots of the brightness-temperature—vs—counts average look-up tables $<T_j(C)>$ for Channels 3, 4, and 5. Table 3 lists the means and Table 4 lists

the standard deviations (from (6)) as a function of count for Channels 3, 4, and 5. The standard deviations σ_{T_j} are not zero for the thermal channels as they are for the visible channels, indicating that some error can be expected from scan to scan in using a "constant" brightness-temperature look-up table, i.e., a look-up table that does not change from scan to scan as the calibration coefficients do. However, the "smallness" of the standard deviations listed in Table 4 indicates that any errors incurred are most often small.

Assuming that the distribution of brightness temperatures to counts is normal for any given 10-bit count value C, then the 1-σ envelope captures 67 percent of the brightness temperatures that would be computed from count C using Eq. (4). The 2-σ envelope captures 95 percent of the brightness temperatures, and the 3-σ envelope captures 99 percent. Thus the $\pm$ 1-σ, 2-σ, and 3-σ envelopes bound the errors incurred 67 percent, 95 percent, and 99 percent of the time using a constant look-up table. It follows that errors greater than 1-σ K can be expected in 3 of every 10 scanlines; errors greater than 2-σ K in 1 of every 20 scanlines; and errors greater than 3-σ K in 1 of every 100 scanlines. Errors of 6-σ K occur from scan to scan $^1/_{100} \times {}^1/_{100}$ (corresponding to a deviation of 3-σ K above the mean in one scan to 3-σ K below the mean in the next scan), or 1 in every 10,000 scanlines.

Table 4 lists the magnitudes and corresponding frequencies of errors for Channels 3, 4, and 5 that can be expected using constant brightness-temperature look-up tables. In general the errors for Channel 3 will be the largest of the three thermal channels 3, 4, and 5; this is related to the fact that Channel 3 also has the lowest signal-to-noise ratio.

Channel 3 1-σ errors are 0.16 K at 320 K, decreasing to a minimum of 0.11 K at 287 K; errors then increase to 0.16 K at 271 K, 0.20 K at 267 K, 0.50 K at 251 K, and to 1.00 K at 240 K. After 240 K, the 1-σ deviations increase rapidly to 50 K at 190 K. However, at 3.7μm the emitted 190 K radiance is $\sim$2 percent of the emitted 320 K radiance. For this reason it is more difficult to measure 3.7μm radiation emitted from very cold bodies (since the signal is small and hence the signal-to-noise ratio is large), which in turn makes it unwise to rely on Channel 3 measurements of very cold (190-230 K) brightness temperatures. The poor accuracy of the Channel 3 measurements for very cold surfaces causes no concern, since Channels 4 and 5 measure the brightness temperatures of such surfaces with a far greater certainty. Channel 3 is most accurate in measuring higher temperatures; it is there that 3.7μm measurements provide the most useful information on clouds.

Both Channels 4 and 5 have much lower errors. Channel 4 1-σ errors decrease monotonically from 0.12 K at 320 K to 0.06 at 190 K. Channel 5 1-σ errors are even smaller, decreasing from 0.05 K at 320 K down to 0.03 at 230 K, and then rising again to 0.05 K at 190 K. Thus for Channels 4 and 5 a very reasonable estimate of brightness temperature can be obtained using constant look-up tables.

NOAA-7 AVHRR Channels 3, 4, and 5 Brightness Temperature Look-up Tables			
Brightness Temperature (°K) <T(C)>	Channel 3 10-bit Count C	Channel 4 10-bit Count C	Channel 5 10-bit Count C
325	-	-	14
320	61	20	70
315	223	83	124
310	361	143	177
305	477	201	228
300	575	257	277
295	657	310	325
290	725	361	370
285	781	410	414
280	826	457	456
275	863	501	497
270	893	543	535
265	917	582	572
260	935	619	607
255	950	655	640
250	962	688	671
245	970	718	701
240	977	747	729
235	982	774	755
230	986	798	779
225	988	821	802
220	989	841	823
215	990	860	842
210	991	877	860
205	991	893	876
200	991	906	891
195	992	919	904
190	992	930	916

Table 3. Average Look-up Tables for NOAA-7 AVHRR Thermal Channels 3, 4, and 5. The mean brightness temperature $<T(C)>$ is given by Eq. (6a) for $j = 3,4,5$

NOAA-7 AVHRR Channels 3, 4, and 5 Look-up Table Standard Deviations									
Temp. (°K)	Errors (Standard Deviations), °K								
	Channel 3			Channel 4			Channel 5		
	1-σ	2-σ	3-σ	1-σ	2-σ	3-σ	1-σ	2-σ	3-σ
325	-	-	-	-	-	-	0.05	0.09	0.14
320	0.16	0.31	0.47	0.12	0.25	0.37	0.04	0.09	0.13
315	0.15	0.29	0.44	0.12	0.24	0.36	0.04	0.08	0.12
310	0.14	0.28	0.42	0.12	0.23	0.35	0.04	0.08	0.12
305	0.13	0.26	0.39	0.11	0.22	0.34	0.04	0.08	0.12
300	0.12	0.24	0.48	0.11	0.22	0.33	0.04	0.08	0.11
295	0.11	0.23	0.34	0.11	0.21	0.32	0.04	0.07	0.11
290	0.11	0.22	0.33	0.10	0.20	0.31	0.04	0.07	0.11
285	0.11	0.22	0.33	0.10	0.20	0.30	0.04	0.07	0.11
280	0.12	0.23	0.35	0.10	0.19	0.29	0.03	0.07	0.10
275	0.14	0.28	0.41	0.09	0.18	0.27	0.03	0.07	0.10
270	0.18	0.35	0.53	0.09	0.18	0.27	0.03	0.06	0.10
265	0.23	0.46	0.69	0.09	0.17	0.26	0.03	0.06	0.09
260	0.30	0.61	0.91	0.08	0.17	0.25	0.03	0.06	0.09
255	0.41	0.82	1.23	0.08	0.16	0.24	0.03	0.06	0.09
250	0.56	1.13	1.69	0.08	0.15	0.23	0.03	0.06	0.09
245	0.75	1.50	2.25	0.07	0.15	0.23	0.03	0.06	0.09
240	1.05	2.10	3.15	0.07	0.14	0.21	0.03	0.06	0.08
235	1.48	2.97	4.45	0.07	0.14	0.20	0.03	0.06	0.09
230	2.32	4.65	6.97	0.07	0.13	0.19	0.03	0.06	0.09
225	11.2	22.4	33.7	0.06	0.13	0.19	0.03	0.06	0.09
220	16.2	32.5	48.5	0.06	0.12	0.18	0.03	0.06	0.09
215	19.2	38.3	57.5	0.06	0.12	0.18	0.03	0.07	0.10
210	22	45	67	0.06	0.12	0.17	0.04	0.07	0.11
205	-	-	-	0.06	0.11	0.17	0.04	0.08	0.11
200	-	-	-	0.06	0.11	0.17	0.04	0.08	0.12
195	-	-	-	0.06	0.11	0.17	0.05	0.09	0.14
190	-	-	-	0.06	0.11	0.17	0.05	0.10	0.15

Table 4. Statistics for the Look-up Tables of the NOAA-7 AVHRR Thermal Channels 3, 4, and 5, Computed Using Eq. (6b). Errors greater than ± 1-σ °K can be expected in 3 of every 10 scanlines; errors greater than ± 2-σ °K in 1 of every 20 scanlines; and errors greater than ± 3-σ °K in 1 of every 100 scanlines

3. EFFECTS OF TRUNCATING THE 10-BIT RAW COUNTS TO 8-, 7-, AND 6-BIT COUNTS (GRANULARITY)

"Granularity" is defined as the change in albedo per 10-bit count for the visible data, and as the change in brightness temperature per 10-bit count for the infrared data. The granularity in albedo or in brightness temperature can be kept small with 10-bit raw counts, since 10-bit counts allow for 1024 possible values of normalized albedoes A_j (which range from 0-100 percent) or 1024 values of brightness temperatures T_j (which range from 190-320 K). Granularity increases when the number of bits retained in the raw counts is decreased (for example, in going from 10-bit down to 8-, 7-, or 6-bit counts). A discussion follows of the effects of truncating the AVHRR 10-bit data stream.

3.1 Visible Data Granularity

Mathematically, granularity for AVHRR visible data is defined as the first derivative of albedo with respect to 10-bit count. Differentiating Eq. (1) with respect to C yields

$$G_{A_j} \equiv \frac{dA_j}{dC} = m_j, \qquad (7)$$

where G_{A_j} is the granularity in units of percent-albedo per 10-bit count; C is the 10-bit visible count; and m_j is the scaled slope value for Channel j in units of percent albedo per 10-bit count. For Channel 1, $m_1 = 0.1068$ percent-albedo/count, so that a change in one 10-bit count corresponds to a change of ~ 0.1 percent-albedo. For Channel 2, $m_2 = 0.1069$ percent-albedo/count, so that a change in one 10-bit count likewise corresponds to a change of ~ 0.1 percent-albedo.

The effect of reducing the raw counts from 10-bits to k-bits is simulated by changing the scaled slope value m_j as follows:

$$m_{j,k} = 2^{10-k}\, m_j, \qquad (8a)$$

where $m_{j,k}$ is the scaled slope value in units of percent albedo per k-bit count; k is the number of bits retained in the raw counts; and m_j is the scaled slope value for 10-bit counts, for Channel j. Replacing Eq. (8a) into Eqs. (1) and (7) gives

$$A_{j,k} = m_{j,k} C_k + b_j, \quad (j = 1,2), \qquad (8b)$$

and

$$G_{A_{j,k}} \equiv \frac{dA_{j,k}}{dC_k} = m_{j,k}, \qquad (8c)$$

where $G_{A_{j,k}}$ is the granularity in units of percent-albedo per k-bit count; $A_{j,k}$ is the percent albedo measured by channel j; $m_{j,k}$ is given by Eq. (8a); C_k is the k-bit count value which ranges from 0 to 2^k-1; and b_j is as for Eq. (1). Note that for $k = 10$, Eqs. (8b) and (8c) reduce to Eqs. (1) and (7), respectively.

Since the slope m_j is positive, the granularity as given by Eq. (8c) is also positive. This is because albedo increases with count. It is also easy to see from Eqs. (8a) and (8c) that the granularity for the visible Channels 1 and 2 increases by a factor of 2 for each bit dropped from the original 10-bit raw count value C. Thus for Channels 1 and 2 the granularity increases from 0.1 percent-albedo per 10-bit count to 0.4, 0.8, and 1.6 percent-albedo per 8-bit ($k = 8$), 7-bit ($k = 7$), and 6-bit ($k = 6$) count, respectively.

3.2 Infrared Data Granularity

Mathematically, granularity for AVHRR thermal data is defined as the first derivative of brightness temperature with respect to 10-bit count. Differentiating Eq. (4c) with respect to C yields

$$G_{T_j} \equiv \frac{dT_j}{dC} = \frac{m_j c_1 c_2 \nu_j^4}{(1+\frac{c_1 \nu_j^3}{m_j C+b_j}) \left[I_j \ln \left(1+\frac{c_1 \nu_j^3}{m_j C+b_j} \right) \right]^2}, \qquad (9)$$

where G_{T_j} is the granularity in units of °K per 10-bit count; C is the 10-bit thermal count; and m_j is the scaled slope value for Channel j in units of $mW/(m^2\ ster\ cm^{-1})$ per 10-bit count. All other variables are as for Eq. (4c). The effect of reducing the raw counts from 10-bits to k-bits is simulated by changing the scaled slope value m_j as follows:

$$m_{j,k} = 2^{10-k}\, m_j, \qquad (10a)$$

where $m_{j,k}$ is the scaled slope value in units of $mW/(m^2\ ster\ cm^{-1})$ per k-bit count; k is the number of bits retained in the raw counts; and m_j is the scaled slope value for 10-bit counts, for Channel j. Replacing Eq. (10a) into Eq. (4c) gives

$$T_{j,k}(C) = \frac{c_2 \nu_j}{\ln \left[1+\frac{c_1 \nu_j^3}{m_{j,k} C_k+b_j} \right]}, \qquad (10b)$$

and replacing Eq. (10a) into Eq. (9) gives

$$G_{T_{j,k}} \equiv \frac{dT_{j,k}}{dC_k} = \frac{m_{j,k} c_1 c_2 \nu_j^4}{\left(1+\frac{c_1 \nu_j^3}{m_{j,k} C_k + b_j}\right)\left[I_j \ln\left(1+\frac{c_1 \nu_j^3}{m_{j,k} C_k + b_j}\right)\right]^2}, \qquad (10c)$$

where $G_{T_{j,k}}$ is the granularity in units of °K per k-bit count; $T_{j,k}$ is the brightness temperature measured by channel j; $m_{j,k}$ is given by (10a); C_k is the k-bit count value which ranges from 0 to 2^k-1; and b_j is as for Eq. (2). All other variables are as for Eq. (4c). Note that for k = 10, (10b) and (10c) reduce to (4c) and (9), respectively. Tables 5a-5c list the granularities for Channels 3, 4, and 5, respectively, as a function of both temperature T and the number of bits k of the raw data (that is 10-bit, 8-bit, 7-bit, or 6-bit counts). Thermal granularities are always negative because $m_{j,k}$ is negative, which is an indication that brightness temperature decreases with increasing count. However, since interest lies in the magnitude of the granularities, their absolute values are listed in Tables 5-7 with the minus sign omitted for simplicity.

As can be seen from Eqs. (9) and (10c), and from Tables 5-7, the granularity for the thermal channels is not constant, unlike the AVHRR visible channels. The absolute temperature differences increase from count to count as brightness temperatures decrease. This is because AVHRR thermal sensors are designed to be most accurate in measuring radiances emitted by warmer surfaces. The exact size of the differences depends on the count C (that is, on the temperature) and also on the AVHRR channel number j. For example, Table 5 shows that for Channel 3 10-bit counts, the brightness temperature T_3 changes from one count to the next by 0.04 K at 310 K; by 0.08 K at 290 K; by 0.18 K at 270 K; and by 0.47 K at 250 K. Compare these changes with those in Table 6 for Channel 4 10-bit counts - the brightness temperature T_4 changes from one count to the next by 0.07 K at 310 K; by 0.08 K at 290 K; by 0.10 K at 270 K; and by 0.13 K at 250 K.

Note too that absolute granularity increases as bits are dropped from the raw counts. Although the granularity is not constant with respect to counts for any of the thermal Channels 3, 4, and 5, it does increase by a constant factor of 2 for each bit dropped from the original 10-bit raw count value C (remember this occurs for the visible channels as well). This is seen by examining (10c); wherever the k-bit count C_k appears, it is multiplied by the weighted slope value $m_{j,k}$. Remember, C_k has been *reduced* by a factor of 2^{10-k}, but $m_{j,k}$ has been *increased* by a factor of 2^{10-k}. Thus their product $m_{j,k}C_k$ remains *constant*, with no net change to $G_{T_{j,k}}$ wherever this product occurs. However in the numerator of (10c), $m_{j,k}$ appears alone; since $m_{j,k}$ increases by a factor of 2^{10-k} (see (10a)), it causes the granularity $G_{T_{j,k}}$ to increase by a factor of 2^{10-k} also. For example, note in Table 7 that for Channel 5 the

Table 5. Granularity for NOAA-7 AVHRR Channel 3, in °K/Count, as a Function of Count Size and Temperature

Temperature (°K)	Channel 3 Granularity (°K/Count)			
	Count Size			
	10-bits	8-bits	7-bits	6-bits
320	0.03	0.11	0.21	0.42
310	0.04	0.15	0.29	0.59
300	0.05	0.21	0.42	0.83
290	0.08	0.30	0.61	1.19
280	0.11	0.46	0.90	1.88
270	0.18	0.70	1.45	2.89
260	0.28	1.14	2.28	4.48
250	0.47	1.82	3.64	7.28
240	0.80	3.19	6.38	12.8
230	1.48	5.39	10.8	21
220	2.53	8.57	17	34
210	6.03	24.1	48	-
200	12.3	48	-	-
190	47.5	-	-	-

granularity is 0.11 K at 270 K for 10-bit counts. It rises to 0.44 K at 270 K for 8-bit counts (an increase of $2^{10-8} = 2^2 = 4$), to 0.88 K at 270 K for 7-bit counts (an increase of $2^{10-7} = 8$), and to 1.75 K at 270 K for 6-bit counts (an increase of $2^{10-6} = 16$).

4. DISCUSSION

4.1 Visible Data

Look-up tables for the AVHRR visible Channels 1 and 2 are very nearly constant from scan to scan. No appreciable error is incurred when using constant look-up tables (Eq. (1)) to convert from counts to normalized albedoes. (For further description, refer to Sections 1.1 and 1.3.1, Table 2, and Figure 1.)

If the visible data is truncated from 10-bit to 6-bit raw counts (a "worst-case" scenario), the granularity increases from ~0.1 percent-albedo per count to ~1.6

Table 6. Granularity for NOAA-7 AVHRR Channel 4, in °K/Count, as a Function of Count Size and Temperature

Temperature (°K)	Channel 4 Granularity (°K/Count)			
	Count Size			
	10-bits	8-bits	7-bits	6-bits
320	0.06	0.26	0.52	1.02
310	0.07	0.28	0.55	1.11
300	0.08	0.30	0.61	1.22
290	0.08	0.33	0.67	1.35
280	0.09	0.37	0.74	1.49
270	0.10	0.41	0.83	1.66
260	0.12	0.47	0.93	1.88
250	0.13	0.53	1.07	2.14
240	0.15	0.62	1.23	2.51
230	0.18	0.73	1.47	2.93
220	0.22	0.87	1.74	3.61
210	0.27	1.06	2.07	4.36
200	0.33	1.36	2.63	5.66
190	0.44	1.79	3.39	6.79

percent-albedo per count. For automated nephanalysis purposes such count-to-count albedo granularities more than likely do not present any difficulty to the quality of the visible data. (For more information, refer to Section 2.1.)

4.2 Infrared Data

Look-up tables for the AVHRR thermal Channels 3, 4, and 5 vary more than the visible look-up tables, as is seen from Tables 3 and 4. Although the errors incurred by using a constant look-up table are usually small, they can become appreciable in size from time to time as previously discussed; these errors are largest for Channel 3. Whether or not these errors are significant depends on the application of the infrared data. For nephanalysis purposes the temperature deviation errors incurred using constant look-up tables for the longwave Channels 4 and 5 will most likely not present any difficulty to the RTNEPH in terms of the quality of that infrared data. However, Channel 3 constant—look-up—table errors can be more significant, especially for brightness temperatures 270 K and lower; it is for this range of temperatures that the Channel 3 sensor is most inaccurate, often requiring updated calibrations on a scan-by-scan basis (See Table 4). In comparison, for multispectral techniques that are sensitive to interchannel differences in brightness temperatures, look-up—table errors can be significant for Channels 4 and 5 as well. For example,

Table 7. Granularity for NOAA-7 AVHRR Channel 5, in °K/Count, as a Function of Count Size and Temperature

Temperature (°K)	Channel 5 Granularity (°K/Count)			
	Count Size			
	10-bits	8-bits	7-bits	6-bits
320	0.07	0.30	0.59	1.18
310	0.08	0.32	0.63	1.26
300	0.09	0.34	0.68	1.36
290	0.09	0.37	0.74	1.47
280	0.10	0.40	0.80	1.62
270	0.11	0.44	0.88	1.75
260	0.12	0.49	0.98	1.97
250	0.14	0.55	1.10	2.21
240	0.16	0.62	1.25	2.55
230	0.18	0.72	1.47	2.93
220	0.21	0.85	1.70	3.29
210	0.25	1.01	2.06	4.13
200	0.31	1.24	2.41	5.11
190	0.38	1.53	3.20	6.41

algorithms using multispectral infrared measurements estimate water vapor amounts using the ratio of Channel 4 and Channel 5 brightness temperatures; this ratio can be quite sensitive to measurement errors of tenths and even hundredths of degrees K. (For further description refer to Sections 1.2 and 1.3.2, Tables 3 and 4, and Figure 2.)

If the thermal data is truncated from 10 bits to 8, 7, or 6 bits then several consequences arise. First, the granularity throughout the temperature scale will be degraded. In going from 10-bit to 6-bit counts (6-bit counts are what the AFGWC Satellite Global Data Base (SGDB) currently retains), the brightness temperature granularity increases by a factor of 16. But more importantly, the accuracy of the brightness-temperature differences among the three thermal channels can also decrease by a factor of 16 or more. The thermal data may be so degraded that it would be difficult for multispectral algorithms to use it effectively. The success of such algorithms is often dependent on small differences in brightness temperature from one thermal channel to the next. (Refer to Section 2.2 and Tables 5a-5c.)

4.3 General Comments

Finally, note that the temperature look-up tables (see Table 3) are not the same among the AVHRR thermal Channels 3, 4, and 5. It should also be noted that the

visible Channels 1 and 2 albedo look-up tables, although nearly the same for NOAA-7, need not necessarily be so similar for other NOAA polar orbiters. In other words, a visible raw count may represent different normalized albedoes. Similarly a given thermal raw count value represents quite different temperatures depending on the channel in which it was measured.

For this reason, if it is desired to intercompare or combine data from two or more of these channels into a single image product a two-step process must take place. First, the raw counts must be converted to brightness temperatures (or albedoes, if data from the visible channels is to be combined) using the appropriate look-up tables. Next, these brightness temperatures (albedoes) can be converted to a common grayshade scale for image processing purposes. Always remember that it is incorrect to combine uncalibrated "raw count" data from two or more of the thermal channels (or from the two visible channels) without first converting the raw counts to brightness temperatures (or normalized albedoes).

In the final analysis, the errors incurred using constant look-up tables or in truncating the original 10-bit raw count data stream will be tolerable for some applications and not for others. The extent to which a high accuracy is needed for measurements of normalized albedoes and brightness temperatures will be driven by individual algorithms and applications. In general, future multispectral techniques that use thermal data will most likely require higher temperature measurement accuracies than the current 6—bit SGDB can support. It is strongly recommended that the AFGWC retain at least 7 and preferably 8 bits of thermal data in both the Satellite Data Handling System (SDHS) and the SGDB.

Appendix A

Average NOAA-7 Slope and Intercept Calibration Coefficients

The average NOAA-7 AVHRR calibration coefficients for the 53497-line sample used in this study are tabulated below:

AVHRR Calibration Coefficients For 10-bit Raw Count Data

Channel	Slope m	Intercept b
1	0.106806	-3.4399
2	0.106905	-3.4882
3	-0.001477	1.4680
4	-0.154670	152.2701
5	-0.180880	177.9360

For the visible Channels 1 and 2, the listed slope can be used for m_j in Eqs. (1), (7), and (8a); the listed intercept can be used for b_j in Eqs. (1) and (8b). The visible slope values are in units of percent-albedo per 10-bit count. The visible intercept values are in units of percent-albedo.

For the thermal Channels 3, 4, and 5, the listed slope can be used for m_j in Eqs. (2), (4c), (9), and (10a); the listed intercept is b_j as for Eqs. (2), (4c), (9), (10b), and (10c). The thermal slope values are in units of $mW/(m^2\ ster\ cm^{-1})$ per 10-bit count. The thermal intercept values are in units of $mW/(m^2\ ster\ cm^{-1})$.

References

1. Kidwell, Catherine B., (1985): **NOAA Polar Orbiter Data (TIROS-N, NOAA-6, NOAA-7, NOAA-8, and NOAA-9) User's Guide.** NOAA/NESDIS, World Weather Building, Room 100, Washington D.C.

2. Lauritson, L., Gary J. Nelson, and Frank W. Porto, (1979): **Data Extraction and *Calibration of* TIROS-N/NOAA Radiometers.** NOAA Technical Memorandum NESS 107, 73pp.